

Numerical Simulations in Cosmology II: Spatial and Velocity Biases

Anatoly Klypin

Department of Astronomy, New Mexico State University, Las Cruces, NM 88001

ABSTRACT

We give a summary of recent results on spatial and velocity biases in cosmological models. Progress in numerical techniques made it possible to simulate halos in large volumes with a such accuracy that halos survive in dense environments of groups and clusters of galaxies. Halos in simulations look like real galaxies, and, thus, can be used to study the biases – differences between galaxies and the dark matter. The biases depend on scale, redshift, and circular velocities of selected halos. Two processes seem to define the evolution of the spatial bias: (1) statistical bias and (2) merger bias (merging of galaxies, which happens preferentially in groups, reduces the number of galaxies, but does not affect the clustering of the dark matter). There are two kinds of velocity bias. The pair-wise velocity bias is $b_{12} = 0.6 - 0.8$ at $r < 5h^{-1}\text{Mpc}$, $z = 0$. This bias mostly reflects the spatial bias and provides almost no information on the relative velocities of the galaxies and the dark matter. One-point velocity bias is a better measure of the velocities. Inside clusters the galaxies should move slightly faster ($b_v = 1.1 - 1.3$) than the dark matter. Qualitatively this result can be understood using the Jeans equations of the stellar dynamics. For the standard LCDM model we find that the correlation function and the power spectrum of galaxy-size halos at $z = 0$ are antibiased on scales $r < 5h^{-1}\text{Mpc}$ and $k \approx (0.15 - 30)h\text{Mpc}^{-1}$.

Subject headings: cosmology: theory - large-scale structure of the universe

1. Introduction

The distribution of galaxies is likely biased with respect to the dark matter. Therefore, the galaxies can be used to probe the matter distribution only if we understand the bias. Although the problem of bias has been studied extensively in the past (e.g., Kaiser 1984; Davis et al., 1985; Dekel & Silk 1986), new data on high redshift clustering and the anticipation of coming measurements have recently generated substantial theoretical progress in the field. The breakthrough in analytical treatment of the bias was the paper by Mo & White (1996), who showed how bias can be predicted in the framework of the extended Press-Schechter approximation. More elaborate analytical treatment has been developed by Catelan et al. (1998ab), Porciani et al. (1998), and Sheth & Lemson (1998). Effects of nonlinearity and stochasticity were considered in Dekel & Lahav (1998) (see also Toruya & Suto (2000)).

Valuable results are produced by “hybrid” numerical methods in which low-resolution N-body simulations (typical resolution $\sim 20\text{kpc}$) are combined with semi-analytical models of galaxy formation (e.g. Diaferio et al. (@; Benson et al. 1999; Somerville et al. 1999). Typically, results of these studies are very close to those obtained with brute-force approach of high-resolution ($\lesssim 2\text{kpc}$) N-body simulations (e.g., Colín et al. 1999a; Ghigna et al. (@). This agreement is quite remarkable because the methods are very different. It may indicate that the biases of galaxy-size objects are controlled by the random nature of clustering and merging of galaxies and by dynamical effects, which cause the merging, because those are the only common effects in those two approaches.

Direct N-body simulations can be used for studies of the biases only if they have very high mass and force resolution. Because of numerous numerical effects, halos in low-resolution simulations do not survive in dense environments of clusters and groups (e.g., Moore, Katz & Lake 1996; Tormen, Diaferio & Syer, 1998; Klypin et al., 1999). Estimates of the needed resolution are given in Klypin et al. (1999). Indeed, recent simulations, which have sufficient resolution have found hundreds of galaxy-size halos moving inside clusters (Ghigna et al., 1998; Colín et al., 1999a; Moore et al., 1999; Okamoto & Habe, 1999).

It is very difficult to make accurate and trustful predictions of luminosities for galaxies, which should be hosted by dark matter halos. Instead of luminosities or virial masses we suggest to use circular velocities V_c for both numerical and observational data. For a real galaxy its luminosity tightly correlate with the the circular velocity. So, one has a good idea what is the circular velocity of the galaxy. Nevertheless, direct measurements of circular velocities of a large complete sample of galaxies are extremely important because it will provide a direct way of comparing theory and observations. This lecture is mostly based on results presented in Colín et al. (1999ab) and Kravtsov & Klypin (1999).

2. Oh, Bias, Bias

There are numerous aspects and notions related with the bias. One should be really careful to understand what what type of bias is used. Results can be dramatically different. We start with introducing the overdensity field. If $\bar{\rho}$ is the mean density of some component (e.g., the dark matter or halos), then for each point \mathbf{x} in space we have $\delta(\mathbf{x}) \equiv [\rho(\mathbf{x}) - \bar{\rho}]/\bar{\rho}$. The overdensity can be decomposed into the Fourier spectrum, for which we can find the power spectrum $P(k) = \langle |\delta_{\mathbf{k}}|^2 \rangle$. We then can find the correlation function $\xi(r)$ and the rms fluctuation of $\delta(R)$ smoothed on a given scale R . We can construct the statistics for each component: dark matter, galaxies, or halos with given properties. Each statistics gives its own definition of bias b :

$$P_h(k) = b_P^2 P_{\delta}(k), \quad \xi_h(r) = b_{\xi}^2 \xi_{\text{dm}}(r), \quad \delta_h(R) = b_{\delta} \delta_{\text{dm}}(R). \quad (1)$$

The three estimates of the bias b are related. In special case, when the bias is linear, local,

and scale independent all three forms of bias are all equal. In general case they are different and they are complicated nonlinear functions of scale, mass of the halos or galaxies, and redshift. The dependence on the scale is not local in the sense that the bias in a given position in space may depend on environment (e.g., density and velocity dispersion) on a larger scale. Bias has memory: it depends on the local history of fluctuations. There is another complication: bias very likely is not a deterministic function. One source of this stochasticity is that it is nonlocal. Dependence on the history of clustering may also introduce some random effect.

There are some processes, which we know create and affect the bias. At high redshifts there is statistical bias: in a Gaussian correlated field high density regions are more clustered than the field itself (Kaiser 1984). Mo & White (1996) showed how the extended Press-Schechter formalism can be used for derivation of the bias of the dark matter halos. In the limit of small perturbations on large scales the bias is (Catelan et al. 1998a; Toruaya & Suto 2000)

$$b(M, z, z_f) = 1 + \frac{\nu^2 - 1}{\delta_c(z, z_f)}. \quad (2)$$

Here $\nu = \delta_c(z, z_f)/\sigma(M, z)$ is the relative amplitude of a fluctuation on scale M in units of the rms fluctuation $\sigma(M, z)$ of the density field at redshift z . Parameter z_f is the redshift of halo formation. The critical threshold of the top-hat model is $\delta_c(z, z_f) = \delta_{c,0}D(z)/D(z_f)$, where D is the growth factor of perturbations and $\delta_{c,0} = 1.69$. At high redshifts, parameter ν for galaxy-size fluctuations is very large and δ_c is small. As the result, galaxy-size halos are expected to be more clustered (strongly biased) as compared to the dark matter. The bias is larger for more massive objects. As fluctuations grow, new forming galaxy-size halos do not represent as high peaks as at large redshifts and the bias tends to decrease. It also loses its sensitivity.

At later stages another process start to change the bias. In groups and cluster progenitors the merging and destruction of halos reduces the number of halos. This does not happen in the field where number of halos of given mass may only increase with time. As the result, the number of halos inside groups and cluster progenitors is reduced relatively to the field. This produces (anti)bias: there is relatively smaller number of halos as compared with the dark matter. This merging bias does not depend on mass of halos and it has a tendency to slow down once a group becomes a cluster with large relative velocity of halos (Kravtsov & Klypin 1999).

Here is a list of different types of biases. We classify them into three groups: (1) measures of bias (2) terms related with the description of biases, (3) physical processes, which produce or change the bias.

- Measures of bias

1. bias measured in a statistical sense (e.g., ratio of correlation functions $\xi_h(r) = b^2\xi_{dm}(r)$)
2. bias measured point-by-point (e.g., $\delta_h(\mathbf{x}) - \delta_m(\mathbf{x})$ diagrams)

- Description of biases
 1. local and nonlocal bias. For example, $b(R) = \sigma_h(R)/\sigma_m(R)$ is the local bias. If $b = b(R; \tilde{R})$, the bias is nonlocal, where \tilde{R} is some other scale or scales.
 2. linear and nonlinear bias. If in $\xi_h(r) = b^2 \xi_{\text{dm}}(r)$ the bias b does not depend on ξ_{dm} , it is the linear bias.
 3. scale dependent and scale independent bias. If b does not depend on scale at which the bias is estimated, the bias is scale independent. Note that in general, the bias can be nonlinear and scale independent, but this highly unlikely.
 4. stochastic and deterministic.
- Physical precesses, which produce or change the bias
 1. statistical bias. Bias, which arises when a specific subset of points is selected from a Gaussian field.
 2. merging bias. Bias produced due to merging and destruction of halos.
 3. physical bias. Any bias due to physical processes inside forming galaxies.

3. Spatial bias

Colín et al. (1999a) have simulated different cosmological models and using the simulations studied halo biases. Most of the results presented here are for currently favored Λ CDM model with the following parameters: $\Omega_0 = 1 - \Omega_\Lambda = 0.3$, $h = 0.7$, $\Omega_b = 0.032$, $\sigma_8 = 1$. The model was simulated with 256^3 particles in a $60h^{-1}\text{Mpc}$ box. Formal mass and force resolutions are $m_1 = 1.1 \times 10^9 h^{-1} M_\odot$ and $2h^{-1}\text{kpc}$. Bound Density Maximum halo finder was used to identify halos with at least 30 bound particles. For each halo we find maximum circular velocity $V_c = \sqrt{GM(< r)/r}$.

In figure 1 we compare the evolution of the correlation functions of the dark matter and halos. There are remarkable differences between halos and the dark matter. The correlation functions of the dark matter always increases with time (but the rate is different on different scales) and it never is a power-law. The correlation functions of the halos at redshifts goes down and then starts to increase again. It is accurately described by a power-law with slope $\gamma = (1.5 - 1.7)$. Figure 2 presents a comparison of the theoretical and observational data on correlation functions and power spectra. The dark matter clearly predicts much too high amplitude of clustering. The halos are much closer to the observational points and predict antibias. For the correlation function the antibias appears on scales $r < 5h^{-1}\text{Mpc}$; for the power spectrum the scales are $k > 0.2h\text{Mpc}^{-1}$. One may get an impression that the antibias starts at longer waves in the power spectrum $\lambda = 2\pi/k \approx 30h^{-1}\text{Mpc}$ as compared with $r \approx 5h^{-1}\text{Mpc}$ in the correlation function. There is no contradiction: sharp bias at small distances in the correlation function when Fourier transformed to the power spectrum produces antibias at very small wavenumbers. Thus, the bias should be taken into account at long

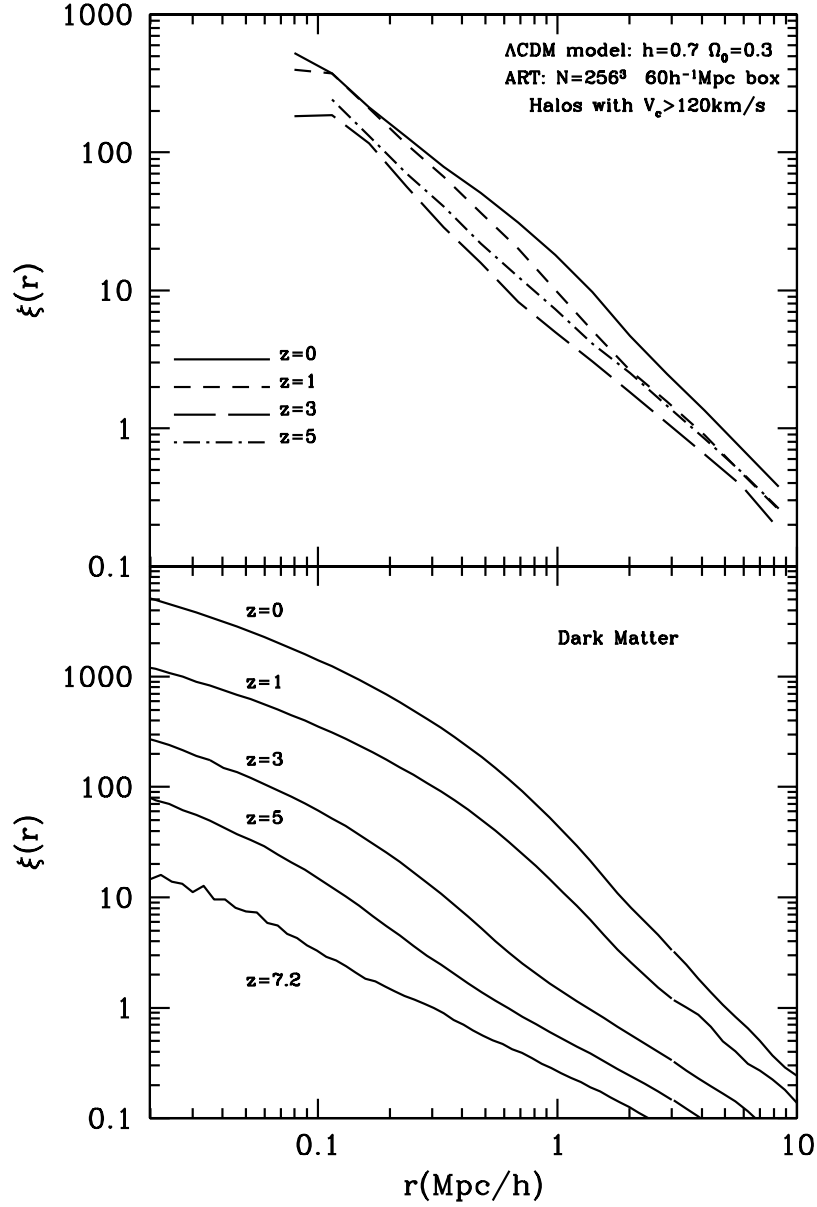


Fig. 1.— Evolution of the correlation function of the dark matter and halos. Correlation function of the dark matter increases monotonically with time. At any given moment it is not a power law. The correlation function of halos is a power-law, but it is not monotonic in time

waves when dealing with the power spectra. There is an inflection point in the power spectrum where the nonlinear power spectrum start to go upward (if one moves from low to high k) as compared with the prediction of the linear theory. Exact position of this point may have been affected by the finite size of the simulation box $k_{\min} = 0.105h^{-1}\text{Mpc}$, but effect is expected to be

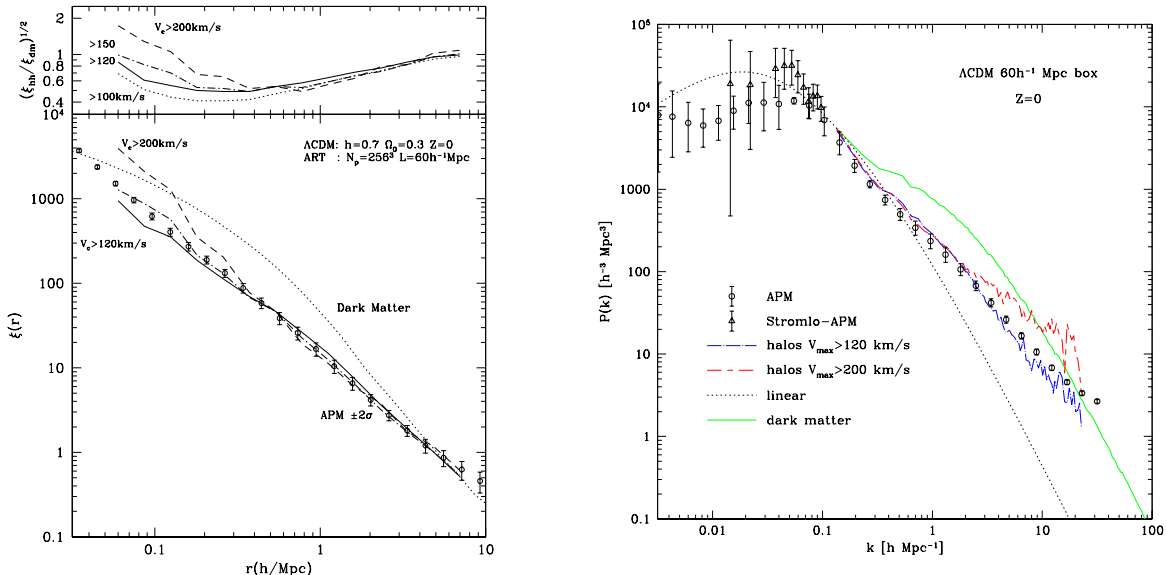


Fig. 2.— The correlation function and the power spectrum of halos of different limiting circular velocities in the Λ CDM model. Results are compared with the observational data from the APM and Stromlo-APM surveys. Bias is scale dependent, but it does not depend much on halo mass

small.

At $z = 0$ the bias almost does not depend on the mass limit of the halos. There is a tendency of more massive halos to be more clustered at very small distances $r < 200h^{-1}\text{kpc}$, but at this stage it is not clear that this is not due to residual numerical effects around centers of clusters. The situation is different at high redshift. At very high redshifts $z > 3$ galaxy-size halos are very strongly (positively) biased. For example, at $z = 5$ the correlation function of halos with $v_c > 150\text{km/s}$ was 15 times larger than that of the dark matter at $r = 0.5h^{-1}\text{Mpc}$ (see Fig.8 in Colín et al. (1999a)). The bias was also very strongly mass-dependent with more massive halos being more clustered. At smaller redshifts the bias was quickly declining. Around $z = 1 - 2$ (exact value depends on halo circular velocity) the bias crossed unity and became less than unity (antibias) at later redshifts.

Evolution of bias is illustrated by Figure 4. The figure shows that at all epochs the overdensity of halos tightly correlates with the overdensity of the dark matter. The slope of the relation depends on the dark matter density and evolves with time. At $z > 1$ halos are biased ($\delta_h > \delta_m$) in overdense regions with $\delta_m > 1$ and antibiased in underdense regions with $\delta_m < -0.5$. At low redshifts there is an antibias at large overdensities and almost no bias at low densities.

Figure 5 shows the density profiles for a cluster with mass $2.5 \times 10^{14} h^{-1}M_\odot$. There is antibias on scales below $300h^{-1}\text{kpc}$. This is an example of the merging and destruction bias. Some of the halos have merged or were destroyed by the central cD halo of the cluster. As the result, there is smaller number of halos in the central part as compared with what we would expect if the number

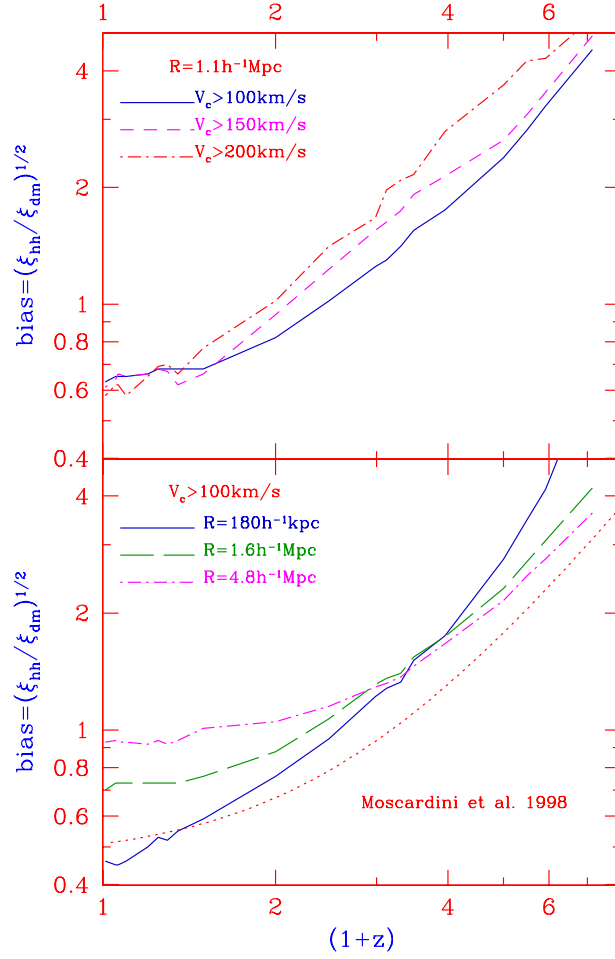


Fig. 3.— *Top panel:* The evolution of bias at comoving scale of $0.54h^{-1}\text{Mpc}$ for halos with different circular velocity. *Bottom panel:* Dependence of the bias on the scale for halos with the same circular velocity.

density of halos follow the density of the dark matter (the full curve in the bottom panel). Note that in the outer parts of the cluster halos closely follow the dark matter.

4. Velocity bias

There are two statistics, which measure velocity biases – differences in velocities of the galaxies (halos) and the dark matter. For a review of results and references see Colín et al. (1999). Two-particle or pairwise velocity bias (PVB) measures the relative velocity dispersion in pairs of objects with given separation r : $b_{12} = \sigma_{\text{halo-halo}}(r) / \sigma_{\text{dm-dm}}(r)$. Figure 6 (left panel) shows this bias. It is very sensitive to the number of pairs inside clusters of galaxies, where relative velocities are largest. Removal of few pairs can substantially change the value of the bias. This “removal” happens when

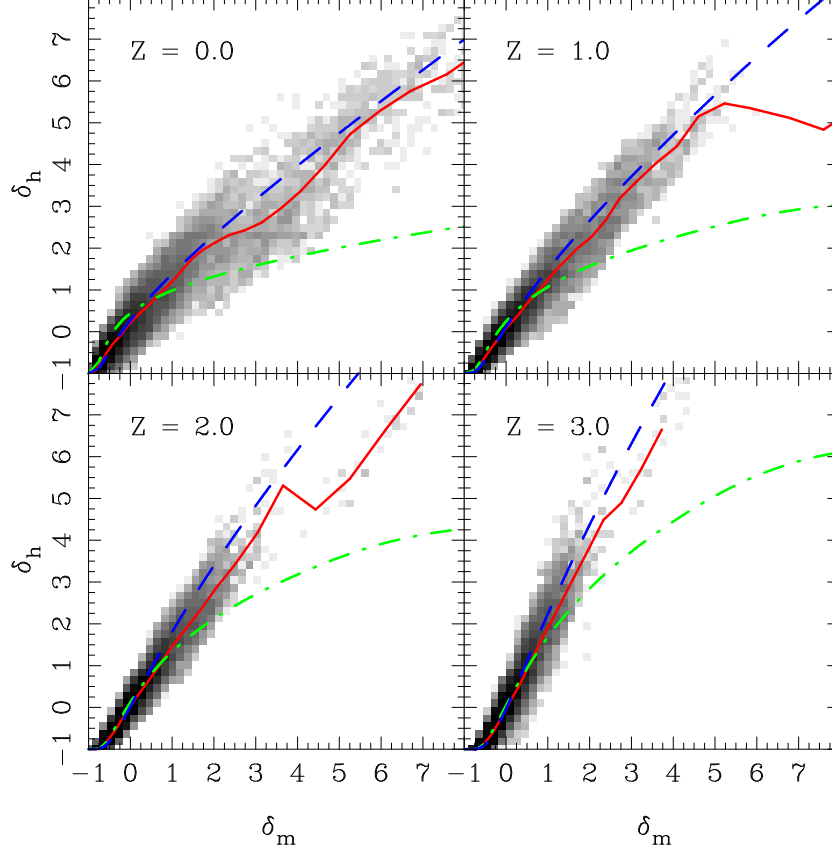


Fig. 4.— Overdensity of halos δ_h vs. the overdensity of the dark matter δ_m . The overdensities are estimated in spheres of radius $R_{\text{TopHat}} = 5h^{-1}\text{Mpc}$. Intensity of the grey shade corresponds to the natural logarithm of the number of spheres in a 2D grid in δ_h - δ_m space. The solid curves show the average relation. The dot-dashed curve is a prediction of an analytical model, which assumes that formation redshift z_f of halos coincides with observation redshift (typical assumption for the Press-Schechter approximation). The long-dashed curve is for model, which assumes that substructure survives for some time after it falls into a larger object: $z_f = z + 1$

halos merge or are destroyed by central cluster halos.

One-point velocity bias is estimated as a ratio of the rms velocity of halos to that of the dark matter: $b_1 = \sigma_{\text{halos}}/\sigma_{\text{dm}}$. It is typically applied to clusters of galaxies where it is measured at different distances from the cluster center. For analysis of the velocity bias in clusters Colín et al. (1999a) have selected twelve most massive clusters in a simulation of the ΛCDM model. The most massive cluster had virial mass $6.5 \times 10^{14}h^{-1}M_{\odot}$ comparable to that of the Coma cluster. The

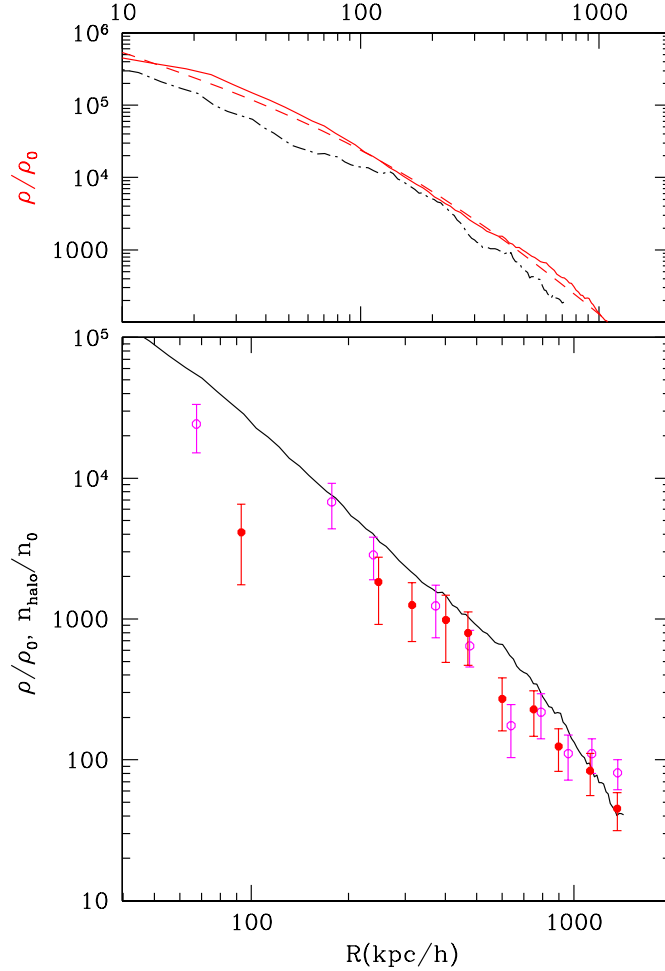


Fig. 5.— Density profiles for a cluster with mass $2.5 \times 10^{14} h^{-1} M_{\odot}$. *Top panel:* Dark matter density in units of the mean matter density at $z = 0$ (solid line) and at $z = 1$ (dot-dashed line). The Navarro-Frenk-White profile (dashed line) provides a very good fit at $z = 0$. The $z = 1$ profile is given in proper (not comoving) units. *Bottom panel:* Number density profiles of halos in the cluster at $z = 0$. (solid circles) and at $z = 1$ (open circles) as compared with the $z = 0$ dark matter profile (solid curve). There is antibias on scales below $300 h^{-1} \text{kpc}$.

cluster had 246 halos with circular velocities larger than 90 km/s. There were three Virgo-type clusters with virial masses in the range $(1.6 - 2.4) \times 10^{14} h^{-1} M_{\odot}$ and with approximately 100 halos in each cluster. Just as the spatial bias, PVB is positive at large redshifts (except for the very small scales) and decreases with the redshift. At lower redshifts it does not evolve much and stays below unity (antibias) at scales below $5 h^{-1} \text{Mpc}$ on the level $b_{12} \approx (0.6 - 0.8)$.

Figure 6 shows one-point velocity bias in clusters at $z = 0$. Note that the sign of the bias is now different: halos move slightly faster than the dark matter. The bias is stronger in the central

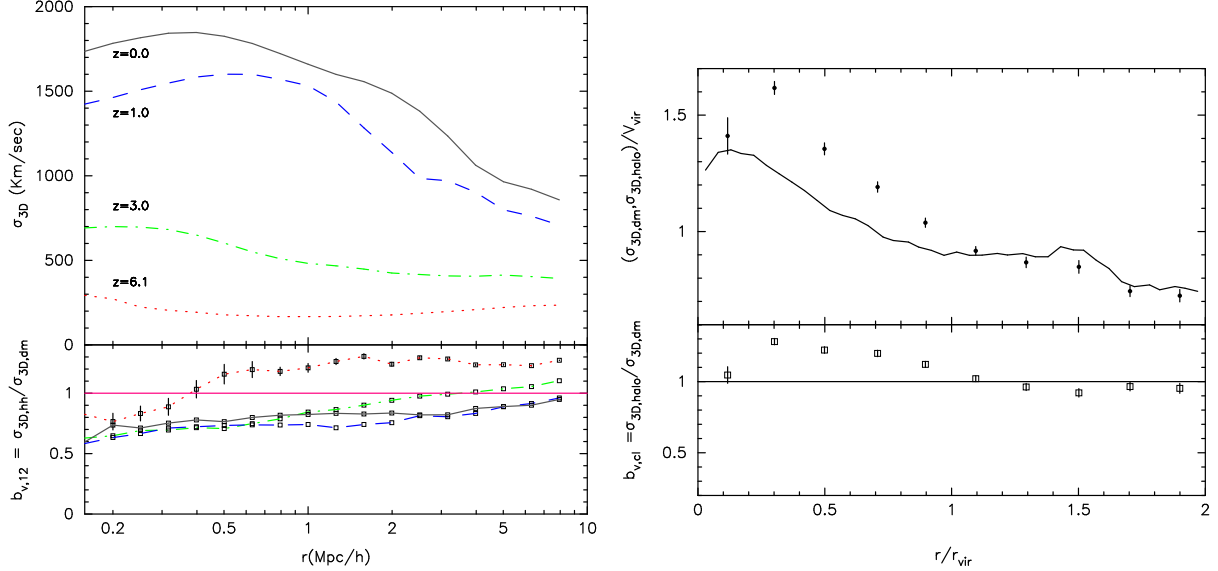


Fig. 6.— *Left*: Two-point velocity bias. *Right: Top panel*: 3D rms velocity for halos (circles) and for dark matter (full curve) in twelve largest clusters. *Bottom panel*: velocity bias in the clusters. The bias in the first point increases to 1.2 if the central cD halos are excluded from analysis. Errors correspond to 1-sigma errors of the mean obtained by averaging over 12 clusters at two moments of time. Fluctuations for individual clusters are larger.

parts $b_1 = 1.2 - 1.3$ and goes to almost no bias $b_1 \approx 1$ at the virial radius and above. Both the antibias in the pairwise velocities and positive one-point bias are produced by the same physical process – merging and destruction of halos in central parts of groups and clusters. The difference is in the different weighting of halos in those two statistics. Smaller number of high-velocity pairs significantly changes PVB, but it does not affect much the one-point bias because it is normalized to the number of halos at a given distance from the cluster center. At the same time, merging preferentially happens for halos, which move with smaller velocity at a given distance from the cluster center. Slower halos have shorter dynamical times and have smaller apocenters. Thus, they have better chance to be destroyed and merged with the central cD halo. Because low-velocity halos are eaten up by the central cD, velocity dispersion of those, which survive, is larger. Another way of addressing the issue of the velocity bias is to use the Jeans equations. If we have a tracer population, which is in equilibrium in a potential produced by mass $M(< r)$, then

$$-r\sigma_r^2(r) \left[\frac{d \ln \sigma_r^2(r)}{d \ln r} + \frac{d \ln \rho(r)}{d \ln r} + 2\beta(r) \right] = GM(< r), \quad (3)$$

where ρ is the number density of the tracer, β is the velocity anisotropy, and σ_r is the rms radial velocity. The r.h.s. of the equation is the same for the dark matter and the halos. If the term in the brackets would be the same, there would be no velocity bias. But there is systematic difference between the halos and the dark matter: the slope of the distribution halos in a cluster $\frac{d \ln \rho(r)}{d \ln r}$ is smaller than that of the dark matter (see Colín et al., 1998, Ghigna et al., 1999). The reason for

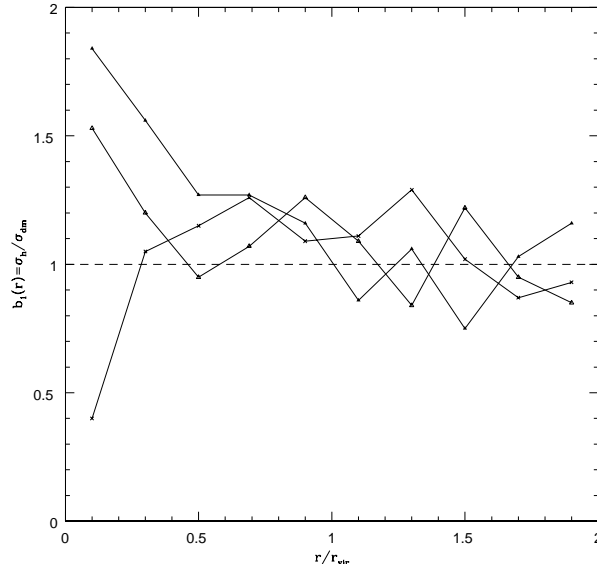


Fig. 7.— One-point velocity bias for 3 Virgo-type clusters in the simulation. Central cD halos are not included. Fluctuations in the bias are very large because each cluster has only ~ 100 halos with $V_c > 90 \text{ km/s}$ and because of substantial substructure in the clusters.

the difference of the slopes is the same – merging with the central cD. Other terms in the equation also have small differences, but the main contribution comes from the slope of the density. Thus, as long as we have spatial antibias of the halos, there should be a small positive one-point velocity bias in clusters and a very strong antibias in pairwise velocity. Exact values of the biases are still under debate, but one thing seems to be certain: one bias does not go without the other.

The velocity bias in clusters is difficult to measure because it is small. The Figure 6 may be misleading because it shows the average trend, but it does not give the level of fluctuations for a single cluster. Note that the errors in the plots correspond to the error of the mean obtained by averaging over 12 clusters and two close moments of time. Fluctuations for a single cluster are much larger. Figure 6 shows results for three Virgo-type clusters in the simulation. The noise is very large because of both poor statistics (small number of halos) and the noise produced by residual non-equilibrium effects (substructure). Comparable (but slightly smaller) value of b_v was recently found in simulations by Ghigna et al. (1999, astro-ph/9910166) for a cluster in the same mass range as in Figure 6. Unfortunately, it is difficult to make detailed comparison with their results because Ghigna et al. (1999) use only one hand-picked cluster for a different cosmological model. Very likely their results are dominated by the noise due to residual substructure. Results of another high-resolution simulation by Okamoto & Habe (1999) are consistent with our results.

5. Conclusions

There is a number of physical processes, which can contribute to the biases. In our papers we explore dynamical effects in the dark matter itself, which result in differences of the spatial and velocity distribution of the halos and the dark matter. Other effects related to the formation of luminous parts of galaxies also can produce or change biases. At this stage it is not clear how strong are those biases. Because there is a tight correlation between the luminosity and circular velocity of galaxies, any additional biases are limited by the fact that galaxies “know” how much dark matter they have.

Biases in the halos are reasonably well understood and can be approximated on a few Megaparsec scales by analytical models. We find that the biases in the distribution of the halos are sufficient to explain within the framework of standard cosmological models the clustering properties of galaxies on a vast ranges of scales from 100 kpc to dozens Megaparsecs. Thus, there is neither need nor much room for additional biases in the standard cosmological model.

In any case, biases in the halos should be treated as benchmarks for more complicated models, which include non-gravitational physics. If a model can not reproduce biases of halos or it does not have enough halos, it should be rejected, because it fails to have correct dynamics of the main component of the Universe – the dark matter.

REFERENCES

- Benson, A.J., Cole, S., Frenk, C.S., Baugh, C.M., & Lacey, C.D. 1999, MNRAS, submitted (astro-ph/9903343)
- Catelan, P., Matarrese, S., & Porciani, C. 1998a, ApJ, 502, 1
- Catelan, P., Lucchin, F., Matarrese, S., & Porciani, C. 1998b, MNRAS, 297, 692
- Colín, P., Klypin, A.A., Kravtsov, A.V., & A.M. Khokhlov. 1999a, ApJ, 523, 32 (astro-ph/9809202)
- Colín, P., Klypin, A., Kravtsov, A. 1999b, ApJ, submitted (astro-ph/9907337)
- Davis, M., Efstathiou, G., Frenk, C.S., & White, S.D.M. 1985, ApJ, 292, 371
- Dekel, A., & Silk, J. 1986, ApJ, 303, 39
- Dekel, A., & Lahav, O. 1998, ApJ, submitted (astro-ph/9806193)
- Diaferio, A., Kauffmann, G., Colberg, J.M., & White, S.D.M., 1998, MNRAS, submitted (astro-ph/9812009)
- Ghigna, S., Moore, B., Governato, F., Lake, G., Quinn, T., Stadel, J. 1998, MNRAS, 300, 146

- Ghigna, S., Moore, B., Governato, F., Lake, G., Quinn, T., Stadel, J. 1999, astro-ph/9910166
- Kaiser, N. 1984, ApJ, 284, L9
- Klypin, A., Gotlöber, S., A.V. Kravtsov, Khokhlov, A. 1999, ApJ, 516, 530
- Kravtsov, A.V., & Klypin, A. 1999, ApJ, 520, 437 (astro-ph/9812311)
- Kravtsov, A.V., Klypin, A., & Khokhlov, A.M. 1997, ApJS 111, 73
- Mo, H.J., & White, S.D.M. 1996, MNRAS, 282, 347
- Moore, B., Katz, N., & Lake, G. 1996, ApJ, 456, 455
- Moore et al., 1999, ApJ, submitted (astro-ph/9907411)
- Okamoto, T., & Habe, A. 1999, ApJ, 516, 591
- Porciani, C., Matarrese, S., Lucchin, F., & Catelan, P. 1998, MNRAS, 298, 1097 (astro-ph/9801290)
- Sheth, R.K., & Lemson, G. 1999, MNRAS, 305, 946 (astro-ph/9808138)
- Somerville, R., Lemson, G., Sigad, Y., Dekel, A., Kauffmann, G., White, S.D.M. 1999, submitted to MN, astro-ph/9912073
- Tormen, G., Diaferio, A., & Syer, D., 1998, MNRAS, 299, 728.
- Toruya, A., & Suto, Y., 2000, astro-ph/0004288